3

Colloidal Hybrid Nanocrystals: Synthesis, Properties, and Perspectives

Jie Zeng[1,2], Xiaoping Wang[1] and J. G. Hou[1]
[1]*Hefei National Laboratory of Physical Science at Microscale, University of Science and Technology of China, Hefei*
[2]*Department of Biomedical Engineering, Washington University, St. Louis*
[1]*P. R. China*
[2]*USA*

1. Introduction

Colloidal nanocrystals are mesoscopic materials occupying the region between the atomistic and the macroscopic worlds.[1] The physical properties of these tiny crystals manifest the transition from molecular limit to the solid state providing benchmark systems for experimental and theoretical studies.[1] In recent years, there have been tremendous developments in the synthetic control of nanocrystal size, shape, and composition, thus allowing the tailoring of their properties.[2-5] These properties, alongside with the ability to manipulate them using the powerful scaffolds of chemical syntheses, also leads to potential applications of colloidal nanocrystals in diverse fields involving physics and biology.[6-11]

A tremendous amount of research in recent years has been directed towards the design and synthesis of multicomponent nanostructures.[5-13] These nanostructures combine two or more components into one solid structure without the use of organic linking molecules, therefore each component is in direct contact with another through one or more of its crystal facets.[14] Such complex structures have the potential to combine magnetic, plasmonic, semiconducting[15] and other physical or chemical properties into a single nanomaterial.[9, 16-17] Efforts to create these multicomponent nanostructures have largely been driven by their increased functionality.[18-19] This increase in function combined with the potential for enhanced, and often tunable, chemical and physical properties makes these nanostructures useful in applications otherwise inaccessible by their single component counterparts.[20] For example, such nanostructures have already found applications in areas such as multimodal biomedical imaging/sensing[21] and photocatalysis.[22-23]

To date, a variety of multicomponent nanostructures have already been successfully synthesized and can be sorted into two groups: *i*) Centrosymmetric structures that are symmetric about a center point, *i.e.* core-shell nanostructures, which most often combine two or more semiconducting materials in order to enhance their photoluminescence;[24] and *ii*) Non-centrosymmetric structures that are asymmetric relative to a center point, *i.e.* hybrid nanostructures.[11, 25-27] In recent years, many research groups have successfully synthesized various multicomponent nanomaterials including semiconductor-semiconductor,[28-29] metal-metal,[30-32] semiconductor-metal,[33-39] and insulator/metal systems[26,40-42] with either a

centrosymmetric structure or non-centrosymmetric structure. This chapter will focus on the non-centrosymmetric hybrid nanostructures. The final structure of these multicomponent materials can take a variety of forms, the most common being that of a "dumbbell" or "matchstick". Another common structure is the heterodimer, which consists of two spherical nanocrystals in intimate contact with each other through selected crystal facets.[43]

Advances in the solution-based synthesis of single component nanostructures have given us the building blocks to create such intricate hybrid nanostructures. It is well known that the properties of single component nanostructures depend greatly on the size and shape of the nanomaterial,[44-45] and that a solution-based synthetic route allows us to access an enormous range of morphologies.[46-55] Likewise, the wet-chemical synthesis of hybrid nanostructures has the potential to create a wide variety of interesting structures.[56-60] Such syntheses will also provide us with the avenues to study the formation mechanisms involved which can in turn be exploited to create targeted multicomponent nanostructures with particular chemical and physical properties. The synthesis of single component nanostructures has been studied for many years and researchers can now manipulate the formation mechanisms involved to produce a desired shape in a high yield. The same formation mechanisms can be useful for the synthesis of some hybrid nanostructures. For example, Ostwald ripening, a well-known mechanism existing in the growth of a crystal, plays a more interesting role in hybrid nanostructure than in single component systems as seen in the synthesis of gold-tipped CdSe nanorods (see Section 2). Due to the increased complexity of hybrid nanostructures, there are many intricate growth mechanisms involved in their syntheses. In addition, the growth mechanisms involved in single-component systems do not always extrapolate to the hybrid nanostructures. In this case, mechanisms such as heterogeneous nucleation and core-shell versus hybrid growth come into play. Further development of the wet-chemical synthesis of hybrid nanostructures will enable us to gain a better understanding of the growth mechanisms involved and learn how to use them to design and synthesize targeted hybrid nanostructures.

The complex structure of hybrid nanostructures offers an interesting system to study how the chemical and physical properties of the individual nanomaterials are affected by the intimate interaction with another component. At the least, multicomponent hybrid nanostructures combine the properties of the individual components independent of each other, creating a multifunctional material.[61] On a higher level, they also have the potential to enhance the inherent properties and possibly even create new ones.[23] For example, Au NPs are usually considered to be catalytically inert. However, when they are combined with a metal oxide compound, *i.e.* Fe_3O_4, the hybrid structure shows high catalytic activity for CO oxidation.[62] This increase in activity arises from the electron transfer from the oxide support to the Fermi level of the adjacent Au NPs.[63-64] In addition, these hybrid nanostructures have been shown to add another parameter with which to finely tune the properties of the individual components.[65-68] For example, Yu and co-workers have demonstrated the ability to tune the UV-vis emission of ZnO-Au nanorods by simply changing the mole ratio between ZnO and the gold precursor, $HAuCl_4$.[67]

In this chapter, we will discuss the growth mechanisms involved in the synthesis of hybrid nanostructures. We will then present a case-study of various hybrid nanostructures that have already been successfully synthesized. Finally, we will detail their physical properties and some of the interesting applications of these multicomponent hybrid nanostructures, followed by perspectives.

2. Mechanisms of the formation of colloidal hybrid nanocrystals

Multiple factors can affect size and shape of nanocrystals produced in a solution through the nucleation and growth process. Taking metallic materials as an example, at the very initial stages, the zero-valence metal atoms form through either reduction of ions or bond breaking of compounds. These metal atoms collide to produce small clusters that are thermodynamically unstable and can dissolve before they reach a critical radius (r^*) or overcome a critical free energy barrier (ΔG^*) and become thermodynamically stable nuclei. These nuclei grow into nanoparticles at the consumption of free atoms in solution or unstable small clusters ($r < r^*$).69 In the classical nucleation theory, the nucleation process can be described according to Gibbs free energy. The excess free energy (ΔG_r), which contains two competing terms, *i.e.* the changes in surface and bulk free energies, reaches the maximum when clusters grow to the critical size. The excess free energy can be described by the following equations.

$$\Delta G_r = 4\pi r^2\gamma + \frac{4}{3}\pi r^3 \Delta G_V = 4\pi r^2\gamma - \frac{4}{3}\pi r^3 \cdot \frac{RTlnS}{V_m} \tag{1}$$

where r is radius of the clusters, γ surface free energy per unit area, R ideal gas constant, ΔG_V change of free energy between solute atoms in solution and bulk crystal per unit volume, T reaction temperature, V_m molar volume of bulk crystal, and S ratio between solute concentrations at saturation and equilibrium conditions. Based on the Eq. (1) and Boltzmann distribution, the number of clusters (N_r) as a function of radius r can be written as:

$$N_r = N_0 \times exp\left(-\frac{\Delta G_r}{RT}\right) \tag{2}$$

where N_0 is the total number of free solute atoms per unit volume. When solute is undersaturated, namely, $S \leq 1$, ΔG_r remains positive and increases with growth of clusters. Nucleation is not favored in such systems. Only when the solute is supersaturated, *i.e.* $S > 1$, ΔG_r can decrease with the increase of cluster radius, and clusters become stable with the growth. The relationship between ΔG_r or N_r and r under the supersaturated condition can be illustrated in Figure 1.

As illustrated in Figure 1A, there is a critical excess free energy, ΔG^*, associated with the critical radius of cluster, r^*. When the radius is smaller than the critical value, the system lowers its free energy by dissolving clusters, and at the same time new ones form due to spontaneous collisions. The expressions of critical radius r^* and maximum excess free energy ΔG^*can then be written as the followings.[69]

$$r^* = -\frac{2\gamma}{\Delta G_V} = -\frac{2\gamma V_m}{RTlnS} \tag{3}$$

$$\Delta G^* = \frac{16\pi\gamma^3 V_m^2}{3(RTlnS)^2} \tag{4}$$

The smaller the critical radius or the maximum excess free energy is, the easier the nuclei form, since the clusters need to incorporate few atoms or overcome a small energy barrier to

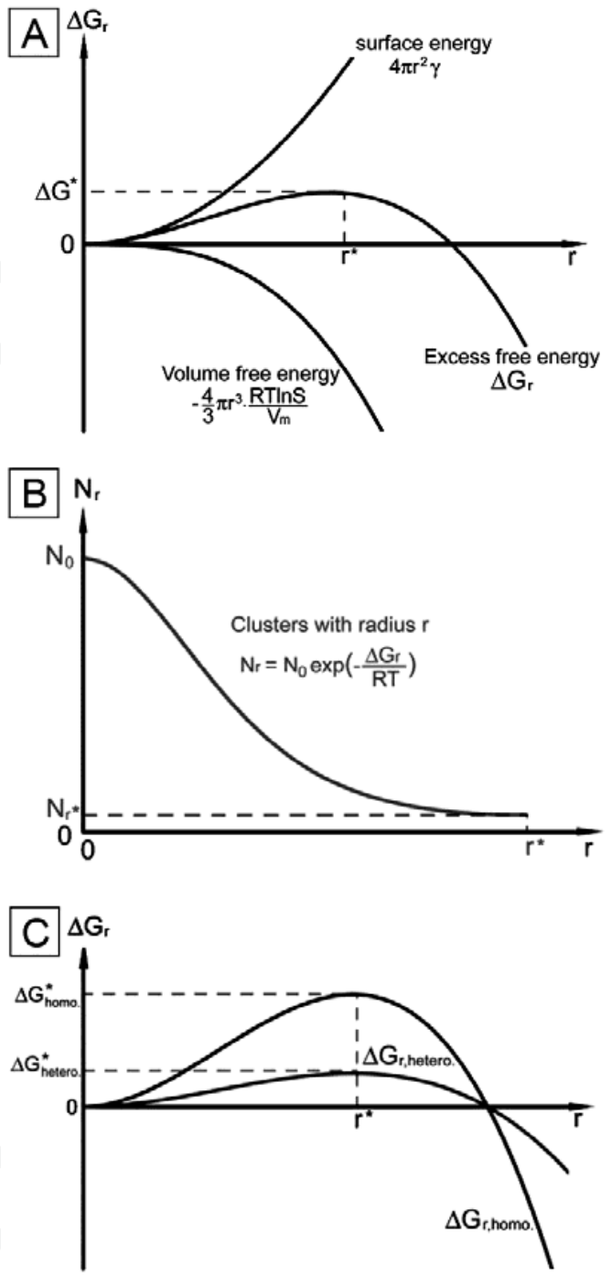

Fig. 1. Illustrations of (A) the generally overall excess free energy, (B) the average number of cluster, and (C) the specifically overall excess free energy for heterogeneous and homogeneous nucleation, as functions of cluster size, respectively.

become stable. Nuclei can hardly form if a reaction system has large values of critical radius or maximum excess free energy. However, when small nanocrystals are present in the system, they can release some of the surface energy through interaction with other species. This interaction changes the subsequent nucleation and growth of clusters. In essence, the critical radius, excess Gibbs free energy, number of nuclei, and rate for a second species formed on existing particles can be described using the following equations.[69-72]

$$r_{hetero}^{*} = -\frac{2\gamma V_m}{RTlnS} \tag{5}$$

$$\Delta G_{hetero}^{*} = \frac{16\pi\gamma^3 V_m^2}{3(RTlnS)^2} \cdot S(\theta) \tag{6}$$

where $S(\theta)$, a numerical value less than unity, is a shape factor describing the geometric relationship between heterogeneous nucleation sites per unit volume. The overall excess free energy (ΔGr) as a function of cluster size (r) for homogeneous and heterogeneous nucleation and growth can be schematically depicted in Figure 1C. The critical energy barrier is generally smaller for heterogeneous nucleation than that for homogeneous one by a factor of $S(\theta)$, while they should have similar critical nucleus radius.

In addition to the theories and equations mentioned above, we can also use the kinetic theory of nucleation, developed based on Gibb's formalism, to describe how the preference for homogeneous nucleation or heterogeneous nucleation is different in different synthetic environments. Using the Arrhenius reaction velocity equation commonly used to determine the rate of a thermally activated process, the rate of nucleation, J, can be expressed as:

$$J = A\exp(-\frac{\Delta G}{kT}) = A\exp\left\{-f\frac{16\pi\Omega^2\gamma_i^3}{3(kT)^3\left[\ln(1+\sigma)\right]^2}\right\},\ 0 < f \le 1 \tag{7}$$

where A is the pre-exponential factor, Ω is the molecular volume, γ_i is the interfacial free energy between the solid nuclei and the liquid phase, and σ is the relative supersaturation. The variable, f, is a parameter describing the influence of foreign bodies on the nucleation energy barrier. For homogeneous nucleation f is equal to 1. Since f can never be greater than 1, heterogeneous nucleation is always kinetically more favorable than homogeneous nucleation. Also, for a given synthetic system where the temperature, T, and the interfacial energy, γ_i, between the two materials are fixed, it can be derived that heterogeneous nucleation will dominate at low supersaturations while homogeneous nucleation is preferred at high supersaturations.[74] In other words, genuine homogeneous nucleation can be regarded as an upper-limit to heterogeneous nucleation in that it requires a very high degree of supersaturation, which may not be easily achieved under standard reaction conditions.[75] Although many models have been proposed over the last few decades to describe the nucleation and growth of small particles,[76-81] we still do not have a thorough understanding of the nature of homogeneous and heterogeneous nucleation, particularly when foreign particles are involved.

Many of the reports concerning the synthesis of multicomponent nanostructures recently have presented either a core-shell or hybrid structure, both of which originate from a heterogeneous nucleation process. Despite this similarity, the details of their epitaxial growth mechanisms are not the same and result in completely different structures.

To reveal the detailed mechanism, realizing the role of lattice mismatch (F) that exists between the deposited material and that in existing seed particles played in the seeded growth processes is definitely important. Note that the size of atoms and the crystallines of these two materials are usually different, and thus leading to specifically preferred arrangements for these materials. Considering material A nucleates on the surface of

material *B* that acts as a seeding particle and provides heterogeneous nucleation sites, the lattice mismatch *F* can be defined as:[81]

$$F = (a_A - a_B) / a_B \tag{8}$$

where a_A and a_B are lattice parameters of growing planes for materials *A* and *B*, respectively. This mismatch induces a positive strain energy (γ_{strain}), which increases rapidly with the growth of nuclei. The larger the mismatch is, the more positive this strain energy becomes. Interfaces formed between metals *A* and *B* during the nucleation and growth, results in a new energy term. The interplay between the interfacial energy (γ_i) and surface energy of these two materials (γ_A and γ_B) may determine the outcome of growth modes. The overall excess energy ($\Delta\gamma$) is created to include the contribution of these four energy terms according to the following equation:[81]

$$\Delta\gamma = \gamma_A + \gamma_i + \gamma_{strain} - \gamma_B \tag{9}$$

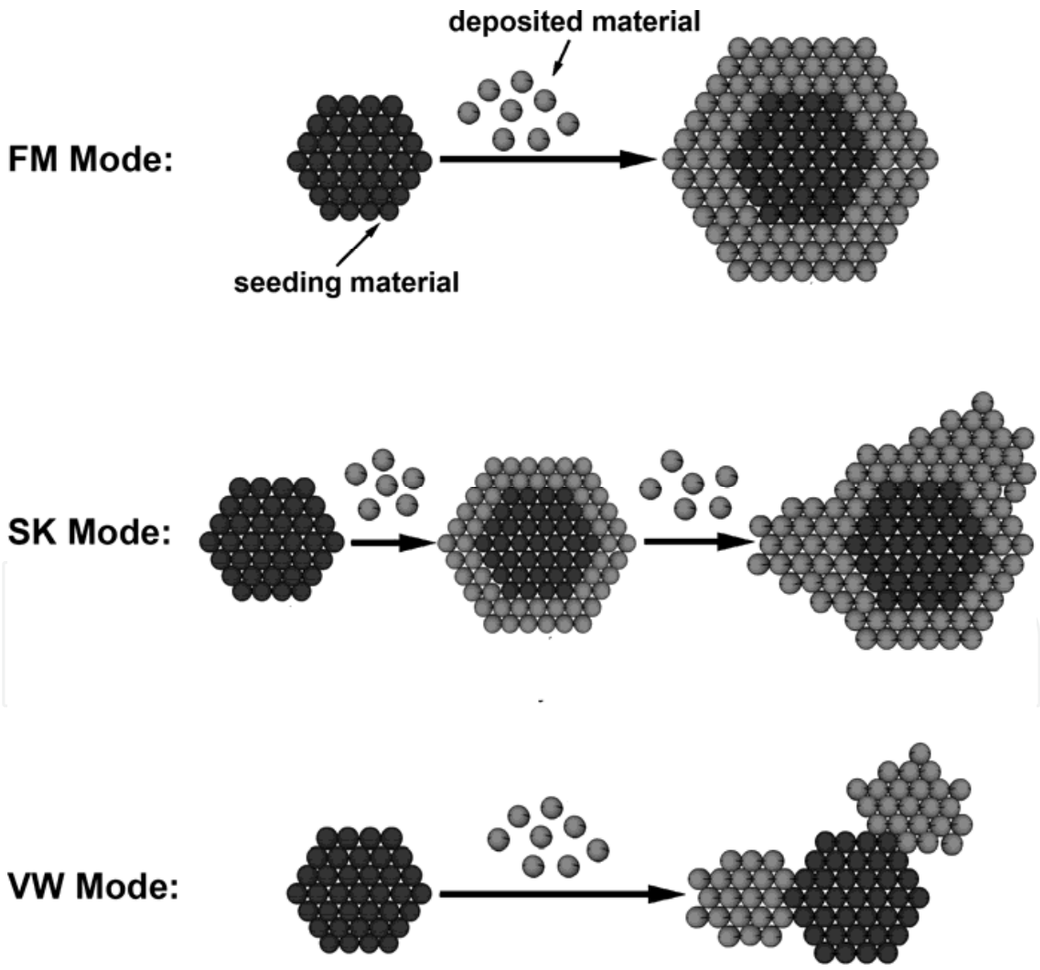

Fig. 2. Schematic illustrations of the FM Mode, the VW Mode, and the SK Mode for the overgrowth of a secondary material on a seed particle. *Courtesy: Nano Today, 2009, 4, 143-164.*

In general, three different types of growth modes can be observed according to the values of overall excess energy $\Delta\gamma$ (Fig. 2).[82] They are: *i*) Frank-van der Merwe (FM) or layer-by-layer Mode, *ii*) Volmer-Weber (VW) or 3D island Mode, and *iii*) Stranski-Krastanow (SK) or 3D island-on-wetting-layer Mode. In the FM Mode, layer-by-layer growth requires that the sum of the surface energy of the deposited material, the strain energy, and the interface energy be less than the surface energy of the seeding material in order for wetting to occur. This means that the value of the overall excess free energy should be negative. On the contrary, if the value of $\Delta\gamma$ is positive, which means the deposition will increase the surface energy of the structure, the layer can lower its total energy by forming isolated, thick 3D islands and can relax the strain by using interfacial misfit dislocations.[83] This type of growth is defined by the SK Mode. It has been demonstrated experimentally that the epitaxial growth of several semiconductor/semiconductor systems with large lattice-mismatches (>~2%) (e.g., Ge/Si,[84-85] InGaAs/GaAs,[86-87] and InGaAs/GaAs[88]) proceeds via the SK Mode.[89] It is found that during layer-by-layer growth the strain energy γ_{strain} increases linearly with the number of strained layers. As a result, when the thickness arrives at a certain point, the sum of γ_i , γ_A, and γ_{strain} exceeds γ_B. At this point the growth mode transforms from the FM Mode to the SK Mode leading to the formation of 3D islands on the 2D wetting layer. This particular type of growth is known as the VW Mode. Those three modes are very useful for predicting and tailoring the growth outcome of multicomponent nanostructures. For example, in order to get a hybrid nanostructure, the overgrowth should satisfy the conditions applied in either the SK Mode or the VW Mode. By doing so, the growth will form isolated 3D islands rather than layers resulting in a hybrid nanostructure instead of a core-shell structure.

In the epitaxial growth of multicomponent nanostructures, many other factors also have an important role in the overgrowth of the secondary phase. For example, a large lattice mismatch prevents the conformal overgrowth of the secondary material. If the lattice mismatch between the two materials is greater than ~5%, the strain energy term will have a large influence making the SK Mode or the VW Mode the preferred growth mode. In addition to the surface energy and lattice mismatch, other factors such as metal bond energy,[90] pH of growth solution,[91] and stirring rate[73] should also be considered in various overgrowth systems.

While these concepts are first developed to explain the film growth, there should not be a fundamental difference between film growth and colloidal synthesis in terms of heterogeneous nucleation. The three growth modes should be able to use, at least in some cases, in understanding the formation of a range of complex nanostructures synthesized in solution phase, such as core-shell and hybrid nanostructures.

Additional considerations need to be taken into consideration during growth of heterogeneous nuclei, which can determine the finial morphology. One key factor is the so-called Ostwald ripening.[92-94] The driving force for this effect arises from the overall energy of the particles involved.[95] In order to lower the total energy of the system, smaller crystallites, which have higher surface energy, dissolve into solution over time. The dissolved species then regrow onto the larger particles.[96-97] This general definition only requires that mass be transferred between particles, however, in other cases both mass and electron transfers are required in order for an Ostwald ripening process to occur.

Banin and co-workers have demonstrated an interesting example of this electrochemical Ostwald ripening process, in which electron transfer was involved across connected particles (Fig. 3).[98] They have developed a series of methods to selectively grow gold

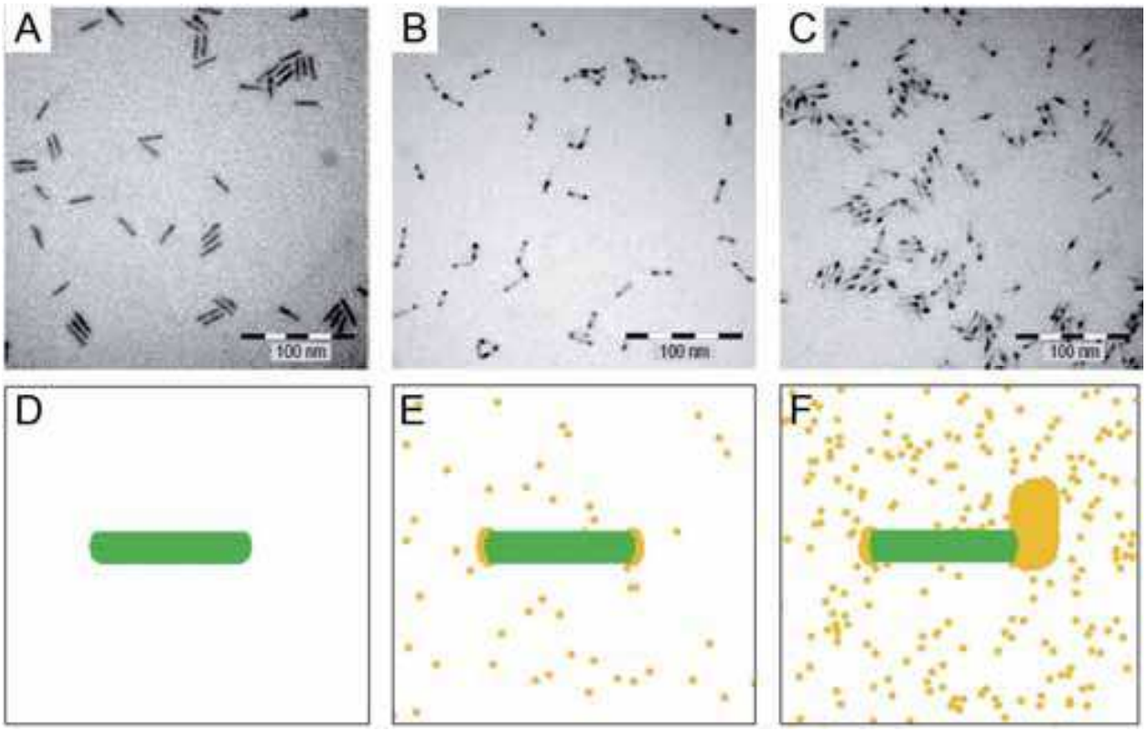

Fig. 3. Effect of increasing Au/rod molar ratio on the growth. Top panels show the experimental results. (A) Original rods of dimension 25×4 nm. (B) "Nano-dumbbells" (NDBs) after adding 1.3 μmol of gold precursors to (A). (C) "Nano-bell-tongues" (NBTs) after adding 1.3 μmol of gold precursors to (B). Lower panels show the theoretical results. (D) Presentation of the system on a two-dimensional lattice. (E) Snapshot of final morphology at low gold concentration (the two-dimensional gold density is 0.001) yielding two-sided growth. (F) Snapshot of final morphology at high gold density (0.01) showing one-sided growth. *Courtesy: Nat. Mater., 2005, 4, 855-863.*

nanoparticles onto the tips of colloidal CdSe nanorods and tetrapods. During the growth of Au-tipped CdSe nanorods, a structural transition from a two-sided "nano-dumbbell" (NDB) to a one-sided "nano-bell-tongue" (NBT) occurs as the gold concentration is increased.[98] They proposed such following process: as the gold precursor in the solution becomes depleted, the thermodynamically stable size for the gold islands increases. Gold islands smaller than this thermodynamically stable size will dissolve back into the growth medium. As gold atoms are oxidized to ions, which can complex with the surfactants in solution, electrons are released into the nanorod. These electrons can then diffuse along the surface of the nanorod to the larger gold particle on the opposite side. The electrons at the second metal tip can then reduce a gold ion from solution, resulting in the overall transport of material from one tip to the other. They observed that during the formation of NBTs no ripening occurs among different NBTs, *i.e.* all of the nanorods have at least one gold tip. They also noticed that no such ripening occurred during the growth of Au-tipped tetrapods. These observations suggest that the electrons are transferred along the semiconductor nanorod rather than through solution. The nanorods transport electrons from the oxidized end to the other so they can reduce the free metal ions in solution. In the case of tetrapods, the large amounts of crystal defects in the central region act as a barrier to the free

movement of electrons, therefore no ripening can occur. Electrochemical Ostwald ripening has been shown previously to only occur on a conductive substrate which facilitates electron transfer from smaller particles to larger ones.[99] Therefore, some kind of conductive pathway is necessary in order for this type of Ostwald ripening to occur.

3. Designer hybrid nanocrystals

In this section, we will review some of the successful approaches that have been reported for the synthesis of hybrid nanoparticles.[100-112]

Sun and co-workers synthesized dumbbell-like Au-Fe_3O_4 nanoparticles by using controlled nucleation of Fe_3O_4 on Au nanoparticles without any pretreatment of the Au surface.[100] The decomposition of $Fe(CO)_5$, followed by room-temperature air oxidation leads to iron nucleation on the surface of the Au nanoparticles and the formation of Au-Fe_3O_4 hybrid nanoparticles. One advantage of this method is that each part of the dumbbell can be manipulated by regulating the synthetic conditions. The size of both the Au component and the Fe_3O_4 component can be controlled up to 20 nm in diameter by changing the ratio between $HAuCl_4$ and OLA, and the ratio between $Fe(CO)_5$ and Au independently. As shown in Figure 4, a Fe_3O_4 (111) plane grows onto an Au (111) plane, giving the dumbbell-like structure. When the solvent was changed from a nonpolar hydrocarbon to slightly polarized diphenyl ether, flower-like Au-Fe_3O_4 hybrid nanoparticles were obtained. Similar flower-like Au-Fe_3O_4 hybrid nanostructures were reported by Grzybowski and co-workers.[113] The Fe_3O_4 component can also be converted to γ-Fe_2O_3 and further to α-Fe_2O_3 under high-temperature annealing conditions. In addition, since Fe_3O_4 can be dissolved while Au stays intact in 0.5 M H_2SO_4 solution, the as-prepared Au-Fe_3O_4 nanoparticles could be etched to form single-component Au nanoparticles and Fe_3O_4 nanoparticles.[114] Similar processes were applied to synthesize Au-MnO nanoflowers reported by Tremel and co-workers[101] where the size and morphology of the nanostructure could be varied by changing the molar ratio of $Mn(acac)_2$ to $Au(Ac)_3$.

Alternatively, heterodimers can be formed by taking advantage of lattice mismatch and selective annealing at relatively low temperatures. Xu and co-workers reported a one-pot synthesic method for generating FePt-CdS hybrid nanostructures.[102] After the growth of the FePt seed particles, elemental S was added to the reaction. The high affinity between the FePt component and elemental S allows S to be deposited on the surface of FePt to form a FePt-S core-shell structure. The subsequent addition of $Cd(acac)_2$, HDD, and TOPO produced metastable FePt-CdS nanoparticles, where CdS was amorphous. Upon further annealing at 280 ^oC, the amorphous CdS crystallized, and the lattice mismatch between FePt and CdS crystals made the core/shell system metastable. This instability led to the formation of the FePt-CdS hybrid nanoparticles, as shown in Figure 5. The extension of this synthesis led to the formation of γ-Fe_2O_3-MS (M=Zn, Cd, Hg) hybrid nanoparticles where γ-Fe_2O_3 nanoparticles were made first and used as seeds.[115]

Recently, our group developed a simple, alternative method to prepare CdSe-Au hybrid nanoparticles as shown in Figure 6.[104] Wurtzite CdSe nanoparticles synthesized using the procedure developed by Peng[116] with some modifications[117-118] were used as seeds. Then a specific amount of a Au(I)-$SC_{12}H_{25}$ (-SR) stock solution mixed with a toluene solution containing the CdSe nanoparticles was reduced by ethylene glycol under agitation. The size of the Au components could be easily tuned by varying the volume ratio of seed solution to Au(I)-SR stock solution. The large lattice mismatch between CdSe and Au (~50%)[119] and the

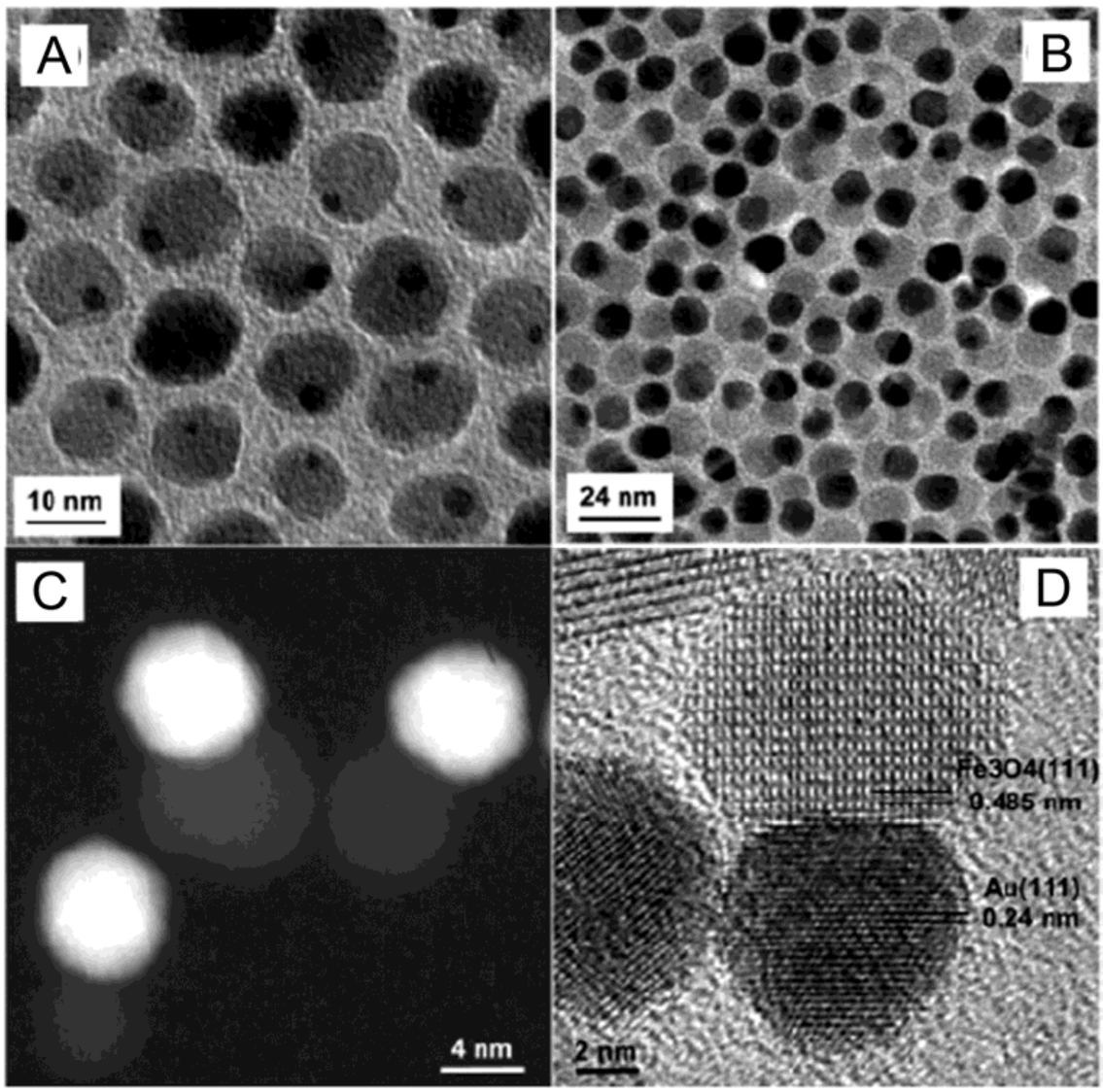

Fig. 4. TEM and STEM images of the dumbbell-like Au-Fe_3O_4 nanoparticles: (A) TEM image of the 3-14 nm Au-Fe_3O_4 particles; (B) TEM image of the 8-14 nm Au-Fe_3O_4 particles; (C) HAADF-STEM image of the 8-9 nm Au-Fe_3O_4 particles; and (D) HRTEM image of one 8-12 nm Au-Fe_3O_4 particle. *Courtesy: Nano Lett., 2005, 5, 379-382.*

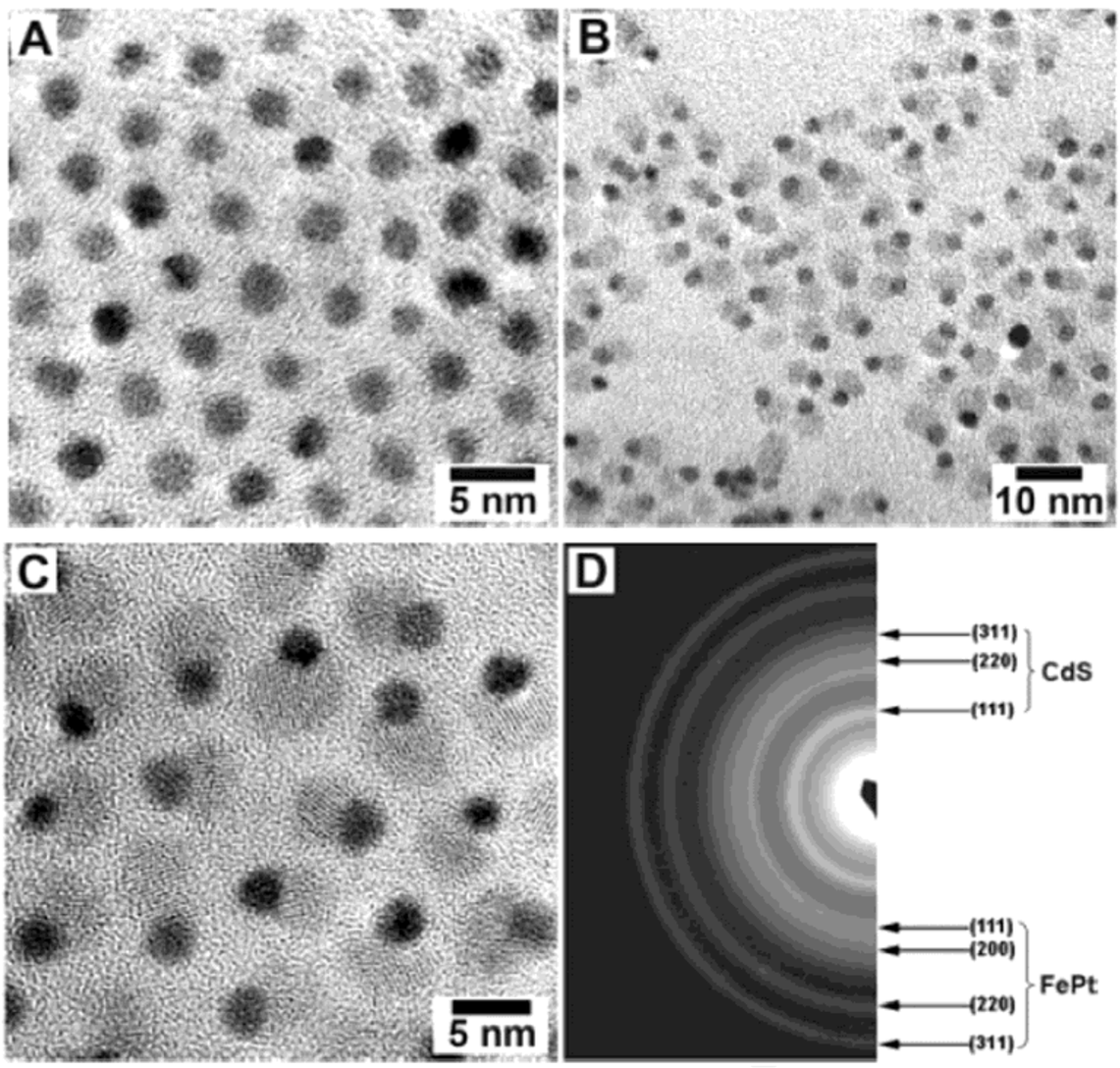

Fig. 5. (A) A TEM image of FePt nanoparticles. Schematic illustration of the synthesis of FePt-CdS hybrid nanoparticles. (B) TEM image of the as-prepared FePt seed particles. (C) TEM image and (D) High-resolution TEM image of the FePt-CdS hybrid nanoparticles. *Courtesy: J. Am. Chem. Soc., 2004, 126, 5664-5665.*

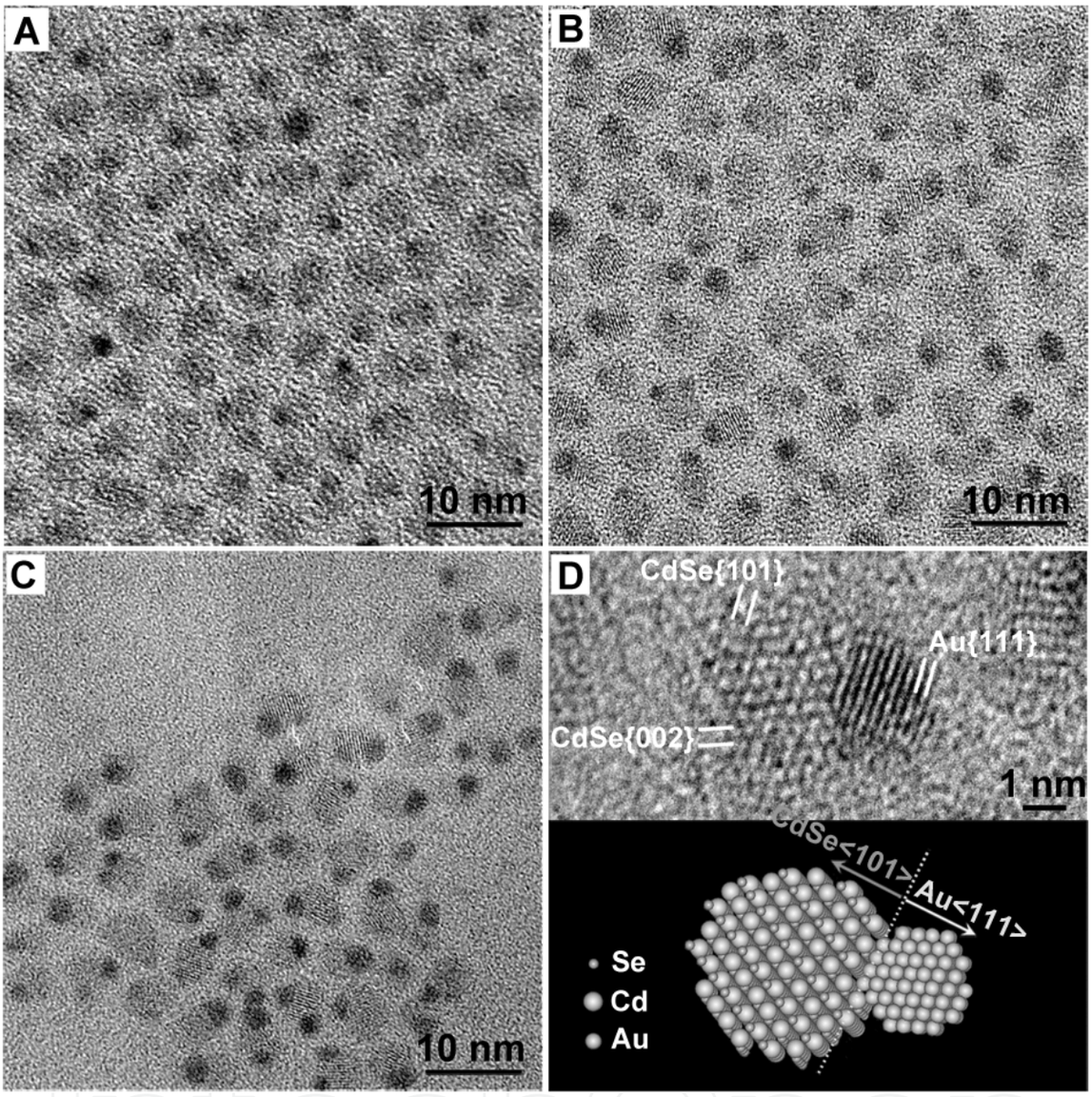

Fig. 6. (A-C) TEM images of CdSe-Au hybrid nanoparticles obtained by changing QAu from 2, 4 to 6 μmol, respectively. The nanoparticles are seen as dimeric units, all with a similar size of ~3.4 nm for the CdSe component. (D) High-resolution TEM image and a schematic drawing of the CdSe-Au hybrid nanoparticles. *Courtesy: Adv. Mater., 2010, 22, 1936-1940.*

self-catalytic reduction of Au(I) ions by the Au clusters prevented the formation of a complete Au shell on the CdSe seed. The surface of the CdSe nanoparticles provided a heterogeneous nucleation site for the formation of Au(0) clusters by simultaneously lowering the energy barrier and serving as a reasonable catalytic site for the reduction of the Au(I)-SR precursor. One important detail in the synthesis we want to emphasize here is the use of a Au(I)-SR complex. This complex has been demonstrated to decompose and serve as an effective source of elemental Au,[120-123] compared to a Au(III) organometallic complex.
Based on the method for the preparation of CdSe-Au hybrid nanoparticles,[104] our group has successfully synthesized PbSe-Au hybrid nanoparticles in which the Au component only

covered one side of the PbSe particle like a cap and the overall shape of the hybrid nanoparticles was similar to a Chinese tumbler (Fig. 7, A and B). In a typical procedure, the Au(I) stock solution, ethylene glycol, and toluene containing the PbSe seed particles were mixed together and heated at 50 ^{o}C for 2 h. The color of the solution changed from green-brown to dark brown gradually, indicating the formation of PbSe-Au hybrid nanoparticles. Besides PbSe-Au, FePt-Au hybrid nanoparticles have also been obtained through the same method (Fig. 7, C and D).

Ying and co-workers reported the synthesis of PbS-Au hybrid nanostructures using a general protocol for transferring metal ions from an aqueous to an organic medium.[109] This process involves mixing an aqueous solution of $HAuCl_4$ with an ethanolic solution of DDA, and then extracting the Au(III) ions into an organic layer to form a Au(III)-DDA compound. Typically, 5 ml of PbS organosol in toluene were mixed with 5 ml of Au(III)-DDA compound in toluene and the mixture was aged for 1 h.

Compared to the growth of CdSe-Au or PbSe-Au nanoparticles, the growth rate of Au particles on Cu_2O seeds reported by our group was found to be much slower.[104] Prior studies have shown that the addition of Ag could facilitate the nucleation and growth of Au nanocrystals, and promote the self-catalyzed reduction of Au ions.[124-125] Therefore, in order to accelerate the reaction, we introduced both a Au(I) stock solution and a Ag(I) stock solution into the system to produce Cu_2O-AuAg hybrid nanoparticles.[104] Cu_2O seeds were prepared by a previously reported procedure.[126] For the synthesis of Cu_2O-AuAg hybrid nanoparticles, Au(I) stock solution and ethylene glycol were added to a light green suspension of Cu_2O seeds. After stirring for 15 min at the room temperature, the Ag(I) stock solution was added. After another 15 min, the solution became purple. The reaction was further continued in air for 2 h, and the products were precipitated with a copious amount of ethanol then collected by centrifugation. As shown in Figure 7, E and F, the shape of the resulting hybrid nanoparticles is between that of a Chinese tumbler and a gourd.

A technique based on performing seeded growth at a liquid/liquid interface under mild conditions was devised to synthesize heterodimers coupling a magnetic section and a noble metal domain.[110] Examples of hybrid nanocrystals synthesized by this biphasic strategy are shown in Figure 8. In the reported procedure, an aqueous metal salt solution was brought in contact with an immiscible organic solvent (such as dichlorobenzene, dichloromethane, hexane, or DOE) in which surfactant-capped γ-Fe_2O_3/Fe_3O_4 or FePt seeds were dissolved. Upon ultrasonic irradiation under inert atmosphere, an emulsion was formed that supposedly consisted of continuous aqueous phase containing "colloidosomes", namely organic microdroplets stabilized by the hydrophobic seeds self-assembled at the organic/water interfaces. The seeding nanocrystals provided catalytic sites onto which the Ag^+ or $AuCl_4^-$ ions were reduced to the respective Ag or Au upon sonication, respectively. As the seeds were only partially exposed to the aqueous phase, metal deposition was spatially restricted to a small surface region and proceeded self-catalytically, thus resulting in a single metal domain on each seed. These hybrid nanocrystals were proven to accommodate a site-differential surface distribution of biomolecules to enable multiple tasks in biomedicine applications.[110] In another recent study, Gu and co-workers have also synthesized similar hybrid nanostructures by mixing FeS-surface-modified Fe_3O_4 nanoparticles and Ag(Ac) in toluene using OA as the capping agent.[111]

Our group has recently reported that by using FePt-CdS heterodimers as the seeds, FePt-CdS-Au ternary hybrid nanoparticles could be obtained by applying the same methodology

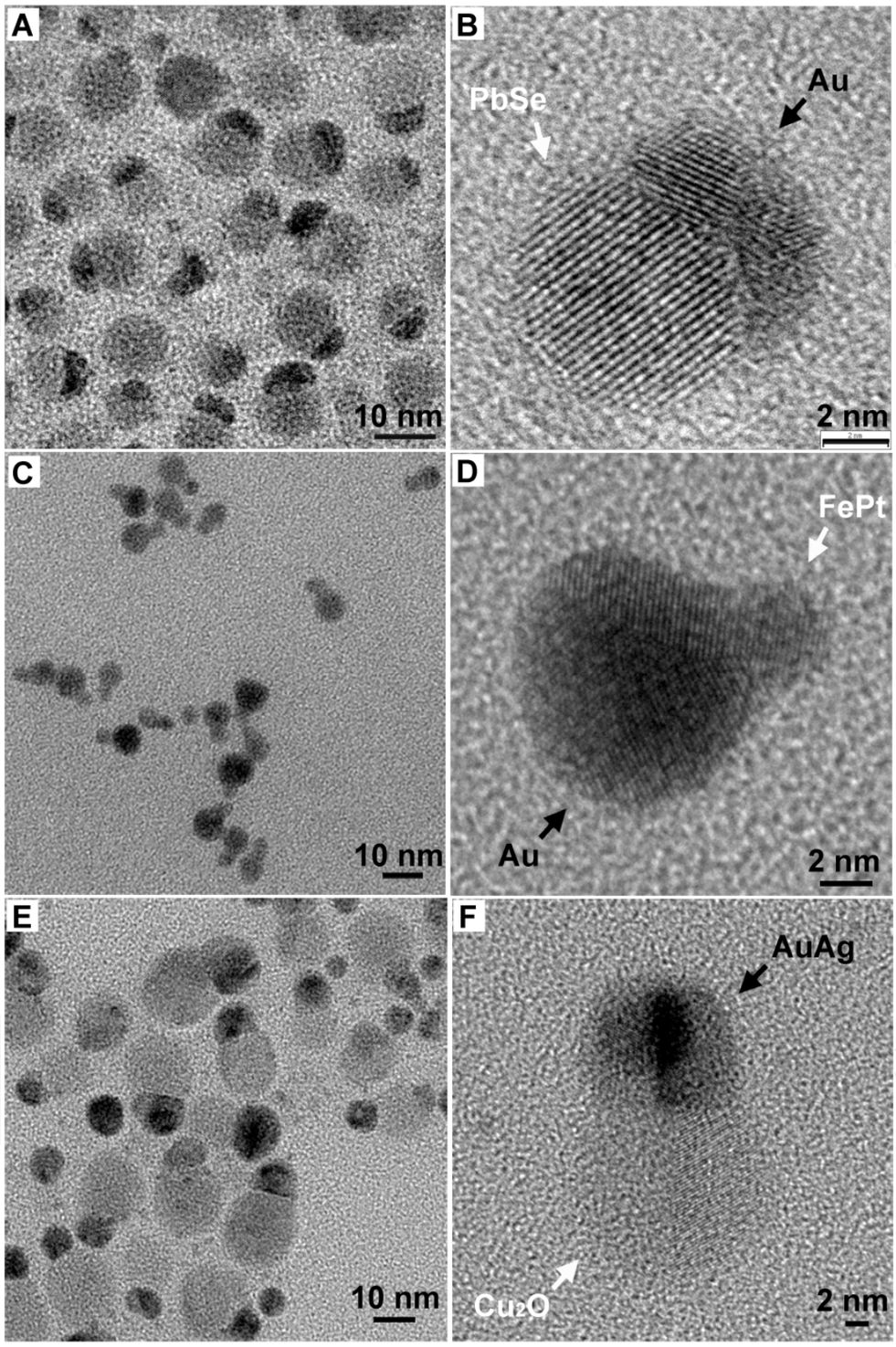

Fig. 7. (A) TEM and (B) high-resolution TEM images of PbSe-Au hybrid nanocrystals. (C) TEM and (D) high-resolution TEM images of FePt-Au hybrid nanocrystals. (E) TEM and (F) high-resolution TEM images of Cu_2O-AuAg hybrid nanocrystals. *Courtesy: Adv. Mater., 2010, 22, 1936-1940.*

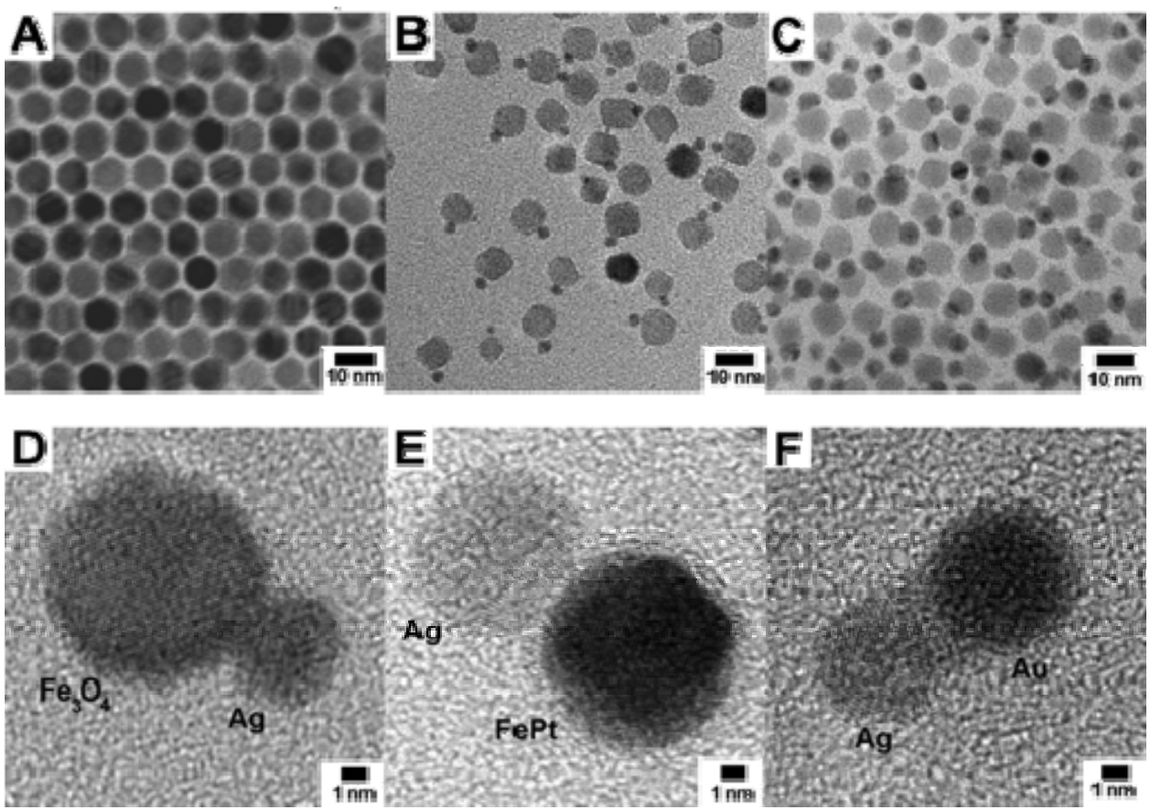

Fig. 8. TEM images of (A) the as-prepared Fe_3O_4 nanoparticles; the Fe_3O_4−Ag heterodimers after (B) 10 min reaction and (C) after reaction stopped at 30 min. HRTEM of (D) Fe_3O_4−Ag heterodimers, (E) FePt−Ag heterodimers, and (F) Au−Ag heterodimers. *Courtesy: J. Am. Chem. Soc., 2005, 127, 34-35.*

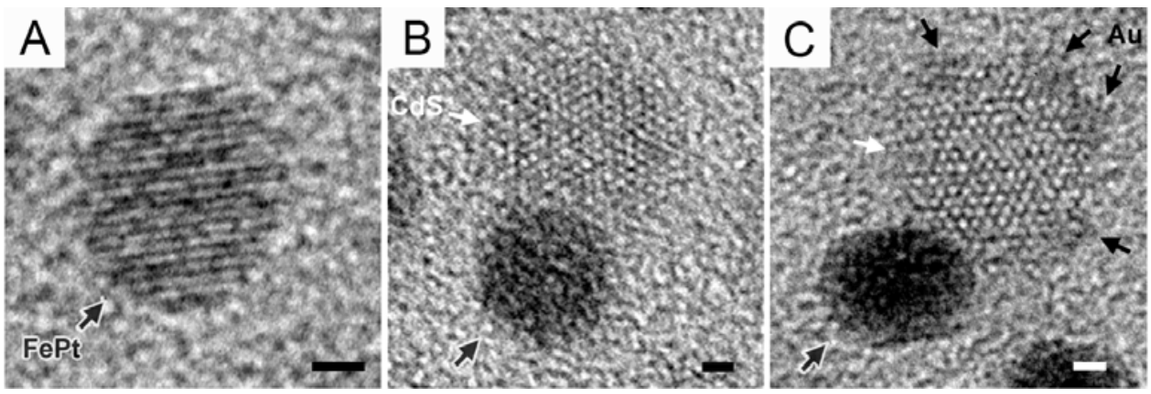

Fig. 9. High-resolution TEM images of (A) FePt, (B) FePt-CdS, and (C) FePt-CdS-Au nanocrystals. All the scale bars correspond to 1 nm. *Courtesy: Adv. Mater., 2010, 22, 1936-1940.*

used in binary systems.[104] In a typical process, two drops of ethylene glycol and a Au(I) stock solution were added to a diluted suspension of FePt-CdS seeds in toluene, and the

mixture was slowly heated to 45 °C and kept for 2 h. As shown in Figure 9, even though both the FePt and the CdS components can act as a catalytic site for the heterogeneous nucleation of Au in a solution, the Au atoms preferred to deposit on the surface of the CdS portion rather than the FePt portion. This observation indicates that there exsits a strong coupling between the two portions of the hybrid seeds, and it significantly impacts on the heterogeneous nucleation process. This coupling effect probably exists widely in binary and multicomponent material systems.

We would like to point out that when spherical seeds (including CdSe, PbSe, and Cu_2O nanoparticles) were used, the hybrid dimeric nanostructures would be the most-commonly observed nanostructures, as shown in Figures, 6 and 7. However, when seed particles with a non-spherical shape were used, such as the CdS-FePt particles, some edge regions on the CdS surface might also provide additional nucleation sites to form nanoparticles with multiple components (Fig. 9C, where four patches of Au were formed on the same particle).

Zeng and co-workers reported a general approach to the synthesis of ternary hybrid nanostructures with a magnetic portion (Fe_3O_4), a metallic portion (Au), and a semiconductor portion (PbSe or PbS).[112] They used binary nanoparticles (specifically, peanut-like Fe_3O_4-Au nanoparticles with 12-nm Fe_3O_4 and 4-nm Au) as seeds. In a typical process, a Pb-oleate complex was formed by mixing PbO, OA and phenyl ether in a 100 mL three-necked flask while heating the mixture at 120 °C. Peanut-like Fe_3O_4-Au nanoparticles in hexane were then injected. After the hexane was removed by distillation, Se-TOP or S-TOP solution was rapidly injected into the reaction mixture at 160 °C. The reaction was quenched by injection of hexane after 1 min. The products are shown in Figure 10. The PbSe/PbS portions were selectively deposited on the surface of the Au portion rather than on the surface of the Fe_3O_4 portion, indicating the great impact of the coupling between two portions of one seed particle on the heterogeneous nucleation process.

The heterogeneous nucleation mechanisms involved in the systems mentioned above suggest that the well-defined structure of the seeds has a great impact on the nucleation and growth of a secondary material. It seems the site with the smallest curvature radius on the seed surface usually acts as the nucleation site for the secondary material because of the high activity at this site. For example, Au particles preferred to form on the tips of CdSe nanorods or tetrapods instead of on their lateral sides. Controlling the nucleation of the secondary material at specific sites on the seeds will help to control the chemical and physical properties of the hybrid nanostructures. However, only a few successful methods have been reported.[127] Our group exploited the use of Cu_2O nanocubes as seeds to accurately position the AuAg clusters during the heterogeneous nucleation process.[104] The experimental observation indicates that the AuAg clusters were formed at all corners of the Cu_2O nanocube.[104] This result further supports the heterogeneous nucleation mechanism described in Section 2. Another successful example has been reported by Yang and co-workers have demonstrated that during the early stages of Pt growth, or at a low Pt concentrations, Pt deposition appeared to occur preferentially only on one tip of the CdS nanorods.[128]

4. Properties and potential applications

One promising application for hybrid nanostructures is in the area of photocatalysis. We take the semiconductor-metal hybrid nanostructures as an example. When semiconductors are irradiated with light greater than their band-gap energy they excite an electron which

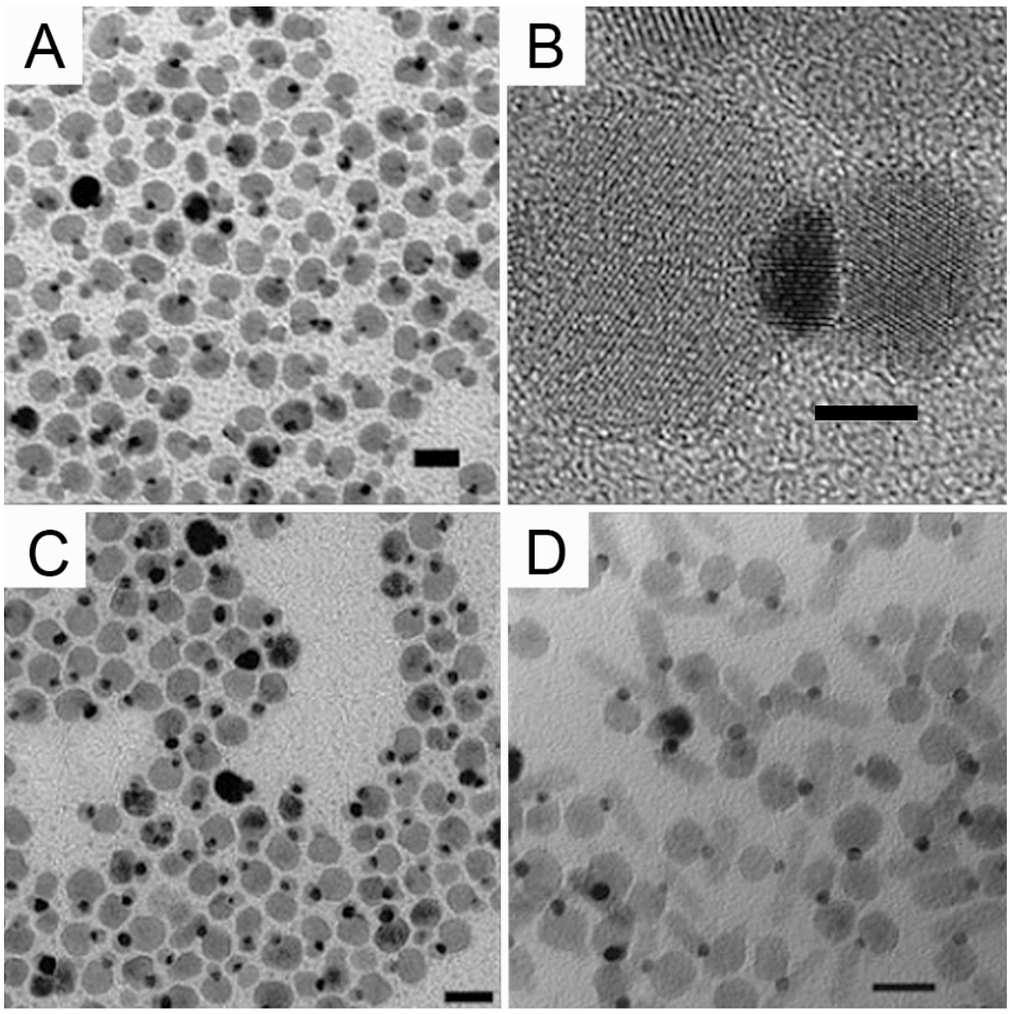

Fig. 10. (A) TEM and (B) High-resolution TEM images of Fe_3O_4-Au-PbSe ternary hybrid nanostructure. (C-D) TEM images of Fe_3O_4-Au-PbS ternary hybrid nanostructure. The scale bars are 20 nm in (A), (C), and (D) and 4 nm in (B). *Courtesy: Nano Lett., 2006, 6, 875-881.*

creates an electron and hole pair. In the case of small nanometer sized particles, the recombination of these pairs occurs on such a rapid time scale that the charges become useless for further redox reactions. To overcome this rapid recombination, researchers deposited a metallic component directly onto the semiconductor nanomaterial in order to aid in charge separation. The metal acts as a charge reservoir which enables the charges to be stored and utilized for a variety of redox reactions. A great example of these particles is the CdSe-Au nanodumbbells synthesized by Banin and co-workers.[23] These particles, when irradiated with visible light, can efficiently separate and store charges for immediate or long-term use in redox reactions (shown in Fig. 11).

In addition to being useful photocatalysts, many multicomponent nanostructures have found application as multimodal biomedical imaging and sensing agents. The increased complexity of these structures allows them to accomplish multiple tasks simultaneously. For example, they can be functionalized with multiple biomolecules by exploiting the different surface chemistries of the components and then used to sense multiple biomarkers

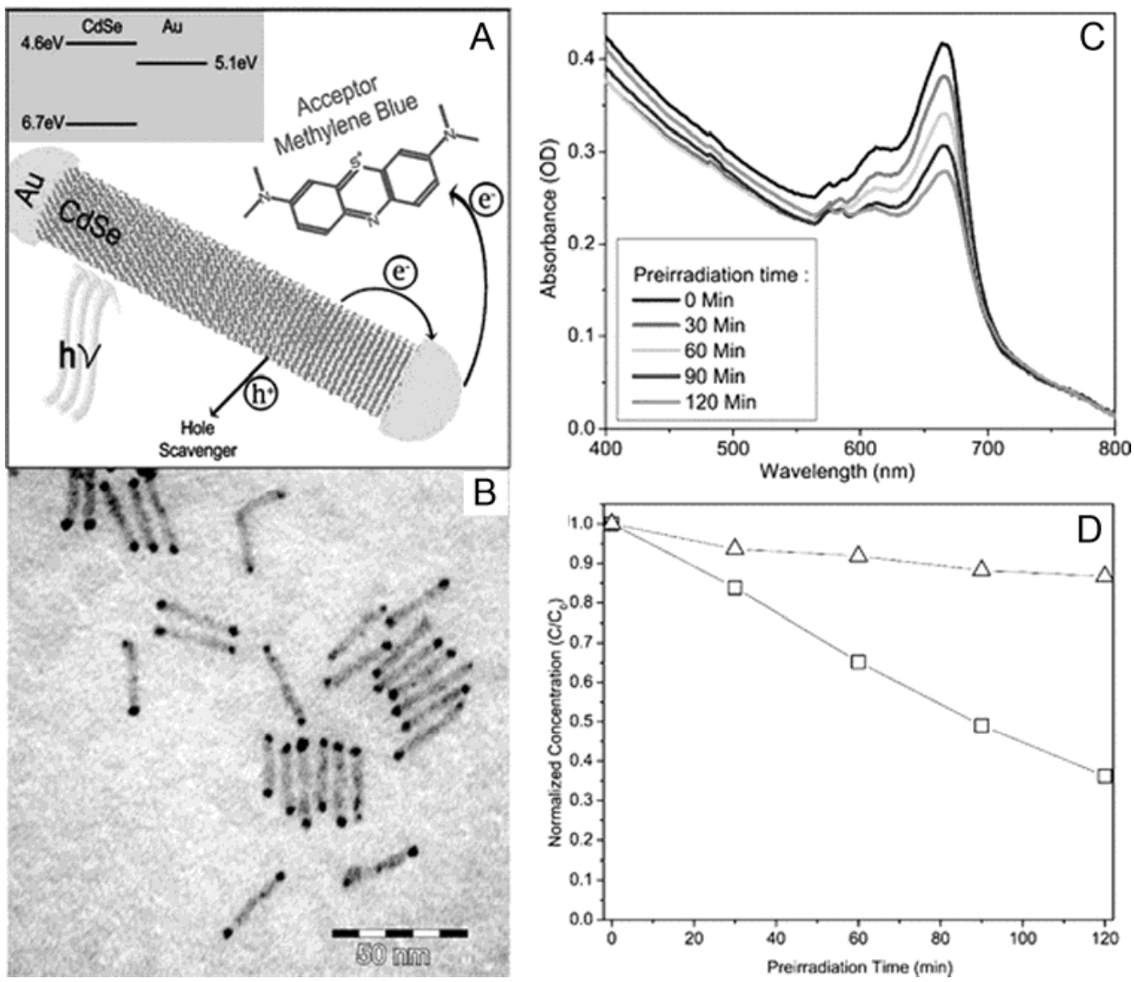

Fig. 11. (A) Scheme of a light-induced charge separation mechanism in a nanodumbbell in which the photogenerated electron−hole pair separates so that the electron resides at the gold tip and the hole at the CdSe nanorod. (B) TEM image of CdSe−Au hybrid nanodumbbells synthesized in aqueous solution. (C) Set of absorbance spectra of methylene blue−nanodumbbells solution in which the double peak absorbance feature of the methylene blue is noticeable, and each spectrum relates to a different pre-irradiation time at 532 nm of the nanodumbbell solution before the addition of the methylene blue. (D) Normalized concentration of methylene blue dye reduced by CdSe nanorods−gold nanoparticles mixture (open blue triangles) and by hybrid CdSe−Au nanodumbbells solution (open black squares) versus pre-irradiation time. *Courtesy: Nano Lett., 2008, 8, 637-641.*

simultaneously. Xu and co-workers have demonstrated this functionality using their Fe_3O_4-Ag hybrid nanostructures.[61] They were able to confirm that they had one molecule bound to the Fe_3O_4 component and another bound to the Ag component. The authors believe that these particles could be useful in areas such as protein binding, molecular imaging and pathogen detection. In addition to having increased imaging and sensing capabilities, the magnetic Fe_3O_4 component adds another degree of functionality to these particles.

Another potential use for hybrid nanocrystals involves the growth of metal tips on one-dimensional semiconductor nanostructures that will serve as integrated electrical contacts to external circuits. A number of strategies have evolved for integrating semiconductor nanorods and nanowires into electrical devices. Typically, nanoscale metal contacts are deposited using electron-beam lithography, focused ion beam deposition, or other methods, onto a nanostructure on a substrate. Metal tips on hybrid nanoparticles may be useful as integrated attachment points to external circuits. The conductance difference present in a metal–semiconductor hybrid nanocrystal is demonstrated in Figure 12, in which gold-tipped CdSe nanorods are characterized using scanning tunneling microscopy (STM).[15] The tip region exhibits lower resistance as compared to the CdSe rod region. In addition, higher tunneling current was observed through the tip, suggesting the tip as a potential electrical contact. The utility of the metal tips for electrical contacts was directly demonstrated by Sheldon and co-workers, who used a trapping method to localize Au-tipped CdSe nanorods between Au electrodes. Transport measurements showed that for CdSe nanorods with gold tips grown in solution, the conductance improved remarkably by five orders of magnitude in comparison to CdSe nanorods.[129] This establishes that hybrid nanostructures allow a path for highly improved electrical connectivity of the semiconductor part to the circuit.

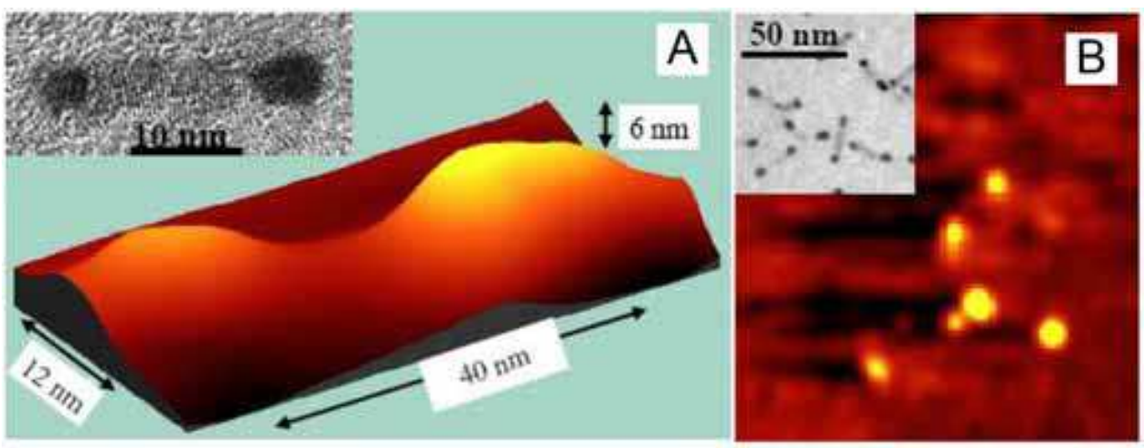

Fig. 12. (A) STM topography image of a single Au-tipped CdSe nanorod (nanodumbbell) taken with V_B = 2 eV. (B) STM current image (150 × 150 nm^2) acquired at a subband gap bias (0.5 eV) showing the gold tips of three nanodumbbells. The insets show high resolution (A) and low resolution (B) TEM images of nanodumbbells. *Courtesy: Phys. Rev. Lett. 2005, 95, 056805.*

The hybrid nanocrystals represent a new set of building blocks as they combine more than one sections with different properties in a single particle. If coupled with biological molecules capable of molecular recognition, these nanocrystals could be chained together through their "anchoring points" (Fig. 13).[95] This could pave the way to assemblies that would behave as nano-machines, equipped, for instance, with magnets for navigation, fluorescent regions that could enable them to be tracked, anchoring regions bearing molecular receptors and chemical releasing agents, and so on. Researchers have already reported substrates bearing a repeating motif of nanocrystals organized in well-defined geometries, which can act as binding sites.[130] Anchoring nanocrystals to these substrates with a high selectivity and in a predictable orientation can be seen as the analogue of the

lock-and-key mechanism that operates in biological systems, and that constitutes the very foundation of self-assembly as realized by nature.[95]

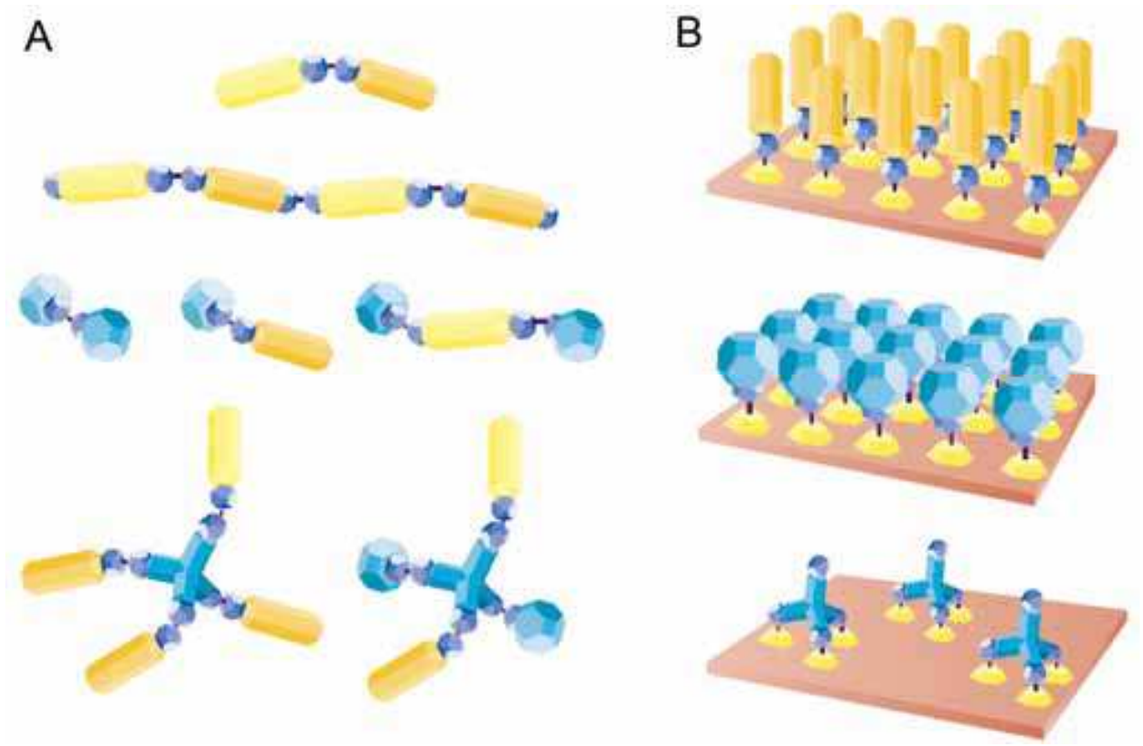

Fig. 13. Strategies for assembly. Nanocrystals carrying anchoring points might be used to build complex nanoscale assemblies, using, for instance, biomolecules as glue. (A) These assemblies could be realized directly in solution, forming, for instance, repeating chains or propeller-like structures. (B) Anchoring of gold-tipped nanocrystals on patterned surfaces is yet another possibility to arrange nanocrystals in programmed locations and orientations *Courtesy: Nat. Mater., 2005, 4, 801-802.*

Grzybowski and co-workers have demonstrated the elegant assembly of Fe_3O_4-Au hybrid nanostructures by extending the concepts of bond strength and steric hindrance to the nanometer regime.[131] In their system, they used a dithiol linker to "react" or aggregate the hybrids. They observed that as they increased the concentration of this linker, the number of hybrid particles per cluster increased. They equated this kind of control to the same kind of control one would have by varying bond strength. Holding the dithiol concentration constant and increasing the size of the bulky Fe_3O_4 domain resulted in a decrease in the number of particles per cluster. This type of control mimics the kind of control observed when varying steric hindrance on the molecular level. By varying these two controls relative to each other, they were able to precisely control the number of hybrid particles in each cluster (Fig. 14).

5. Perspectives

This chapter presents many of the diverse types of colloidal hybrid nanocrystals that have been achieved over the last several years. While the range of material combinations,

geometries, and properties that have been presented is impressive, this area of study still remains challenges in industry applications. One challenge is to optimize the growth conditions and thus to obtain hybrid nanocrystals with well-defined structures and

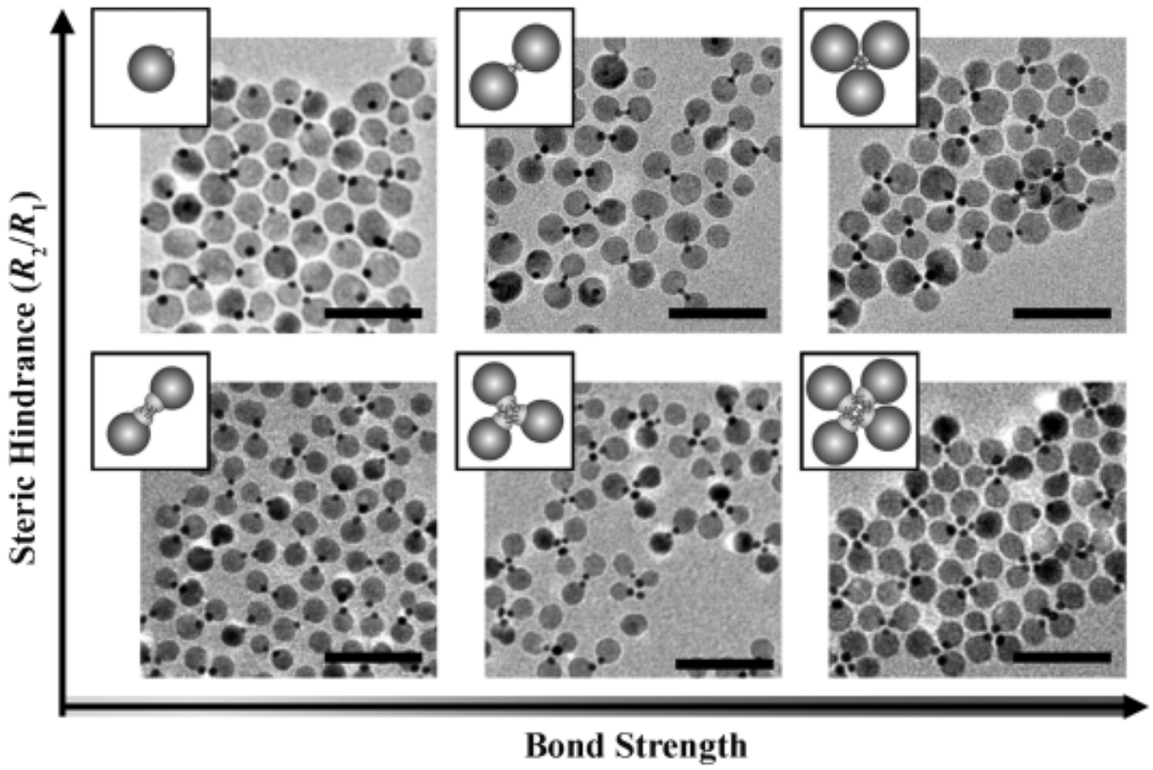

Fig. 14. TEM images of nanoclusters obtained for different bond strengths (determined by the dithiol concentration) and steric hindrance (quantified by the ratio, $s=R_2/R_1$). The insets provide a schematic illustration of the most probable nanoparticle cluster. The images correspond to dithiol concentrations of 0.3 M, 5 M, and 500 M (left to right) and s of 2.9 and 3.8 (bottom and top, respectively). All scale bars are 50 nm. *Courtesy: Angew. Chem. Int. Ed., 2009, 48, 9477-9480.*

controllable physical properties. Since sufficient strategies for fabricating hybrid nanocrystals have been developed, a coherent picture of how reaction conditions and material combinations would be tuned to influence the growth mechanism of the hybrid nanocrystals is yet to emerge. As these strategies become more robust, a diverse library of material combinations, arranged in different geometries, will provide insight into the interaction of different material systems at the nanometer scale.[132] Prospectively, such material combinations may lead to multiple functions, such as luminescence associated with catalysis. Contact points on the hybrids may allow further development of bottom-up assembly strategies for constructing complex electrical and optical devices, such as those for solar energy harvesting. Applications in other fields, such as spintronics or biological probes, need to be demonstrated upon development of specific hybrid systems. Although such explorations are still in an very early stage, the ability to tune the properties or impart multiple functionalities to hybrid nanocrystals shows high potential for their future inclusion in emerging modern technologies.

6. Acknowledgement

This work is supported by NSFC under Grant Nos. 50721091, 90921013 and 11074231 as well as by Chinese Academy of Sciences (CAS) and MOST of China (2011CB921403). J.Z. also acknowledges the financial support from the CAS (the startup fund of the outstanding doctoral dissertation award of CAS).

7. References

[1] P. D. Cozzoli, T. Pellegrino and L. Manna, *Chem. Soc. Rev.*, 2006, 35, 1195-1208.
[2] W. Shi, H. Zeng, Y. Sahoo, T. Y. Ohulchanskyy, Y. Ding, Z. L. Wang, M. Swihart and P. N. Prasad, *Nano Lett.*, 2006, 6, 875-881.
[3] H. Zeng and S. Sun, *Adv. Funct. Mater.*, 2008, 18, 391-400.
[4] R. Hao, R. Xing, Z. Xu, Y. Hou, S. Gao and S. Sun, *Adv. Mater.*, 2010, 22, 2729-2742.
[5] Y. Wu, J. Xiang, C. Yang, W. Lu and C. M. Lieber, *Nature*, 2004, 430, 61-65.
[6] D. Wang and Y. Li, *J. Am. Chem. Soc.*, 2010, 132, 6280-6281.
[7] R. D. Robinson, B. Sadtler, D. O. Demchenko, C. K. Erdonmez, L.-W. Wang and A. P. Alivisatos, *Science*, 2007, 317, 355-358.
[8] F. Wurm and A. F. M. Kilbinger, *Angew. Chem. Int. Ed.*, 2009, 48, 8412-8421.
[9] X. Peng, M. C. Schlamp, A. V. Kadavanich and A. P. Alivisatos, *J. Am. Chem. Soc.*, 1997, 119, 7019-7029.
[10] W. C. W. Chan and S. Nie, *Science*, 1998, 281, 2016-2018.
[11] P. D. Cozzoli, T. Pellegrino and L. Manna, *Chem. Soc. Rev.*, 2006, 35, 1195-1208.
[12] Y. Yin and A. P. Alivisatos, *Nature*, 2005, 437, 664-670.
[13] M. Casavola, V. Grillo, E. Carlino, C. Giannini, F. Gozzo, E. F. Pinel, M. A. Garcia, L. Manna, R. Cingolani and P. D. Cozzoli, *Nano Lett.*, 2007, 7, 1386-1395.
[14] S. Kinge, M. Crego-Calama and D. N. Reinhoudt, *ChemPhysChem*, 2008, 9, 20-42.
[15] D. Steiner, T. Mokari, U. Banin and O. Millo, *Phys. Rev. Lett.*, 2005, 95, 056805.
[16] I. L. Medintz, H. T. Uyeda, E. R. Goldman and H. Mattoussi, *Nat. Mater.*, 2005, 4, 435-446.
[17] V. Subramanian, E. E. Wolf and P. V. Kamat, *J. Phys. Chem. B*, 2003, 107, 7479-7485.
[18] M. Green, *Small*, 2005, 1, 684-686.
[19] H. Y. Lin, Y. F. Chen, J. G. Wu, D. I. Wang and C. C. Chen, *Appl. Phys. Lett.*, 2006, 88, 161911-161913.
[20] S. Deka, A. Falqui, G. Bertoni, C. Sangregorio, G. Poneti, G. Morello, M. D. Giorgi, C. Giannini, R. Cingolani, L. Manna and P. D. Cozzoli, *J. Am. Chem. Soc.*, 2009, 131, 12817-12828.
[21] J. Choi, Y. Jun, S. Yeon, H. C. Kim, J. Shin and J. Cheon, *J. Am. Chem. Soc.*, 2006, 128, 15982-15983.
[22] P. V. Kamat, *J. Phys. Chem. C*, 2007, 111, 2834-2860.
[23] R. Costi, A. E. Saunders, E. Elmalem, A. Salant and U. Banin, *Nano Lett.*, 2008, 8, 637-641.
[24] X. Wang, X. Ren, K. Kahen, M. A. Hahn, M. Rajeswaran, S. Maccagnano-Zacher, J. Silcox, G. E. Cragg, A. L. Efros and T. D. Krauss, *Nature*, 2009, 459, 686-689.
[25] C. Wang, C. Xu, H. Zeng and S. Sun, *Adv. Mater.*, 2009, 21, 3045-3052.
[26] A. Perro, S. Reculusa, S. Ravaine, E. B. Bourgeat-Lami and E. Duguet, *J. Mater. Chem.*, 2005, 15, 3745-3760.
[27] S. C. Glotzer and M. J. Solomon, *Nat. Mater.*, 2007, 6, 557-562.

[28] B. O. Dabbousi, J. RodriguezViejo, F. V. Mikulec, J. R. Heine, H. Mattoussi, R. Ober, K. F. Jensen and M. G. Bawendi, *J. Phys. Chem. B*, 1997, 101, 9463-9475.
[29] M. A. Hines and P. Guyot-Sionnest, *J. Phys. Chem.*, 1996, 100, 468-471.
[30] E. Cho, P. Camargo and Y. Xia, *Adv. Mater.*, 2010, 22, 744-748.
[31] F. Fan, D. Liu, Y. Wu, S. Duan, Z. Xie, Z. Jiang and Z. Tian, *J. Am. Chem. Soc.*, 2008, 130, 6949-6951.
[32] P. H. C. Camargo, Y. Xiong, L. Ji, J. M. Zuo and Y. Xia, *J. Am. Chem. Soc.*, 2007, 129, 15452-15453.
[33] V. Subramanian, E. Wolf and P. V. Kamat, *J. Phys. Chem. B*, 2001, 105, 11439-11446.
[34] T. Mokari, E. Rothenberg, I. Popov, R. Costi and U. Banin, *Science*, 2004, 304, 1787-1790.
[35] P. X. Gao, C. S. Lao, Y. Ding and Z. L. Wang, *Adv. Funct. Mater.*, 2006, 16, 53-62.
[36] Y. Lei and W. K. Chim, *J. Am. Chem. Soc*, 2005, 127, 1487-1492.
[37] Z. Sun, Z. Yang, J. Zhou, M. Yeung, W. Ni, H. Wu and J. Wang, *Angew. Chem. Int. Ed.*, 2009, 48, 2881-2885.
[38] Y. Wang, M. Li, H. Jia, W. Song, X. Han, J. Zhang, B. Yang, W. Xu and B. Zhao, *Spec. Acta A–Mol. Biomol. Spec.*, 2006, 64, 101-105.
[39] J. Yang, H. I. Elim, Q. B. Zhang, J. Y. Lee and W. Ji, *J. Am. Chem. Soc.*, 2006, 128, 11921-11926.
[40] M. Lahav, E. A. Weiss, Q. B. Xu and G. M. Whitesides, *Nano Lett.*, 2006, 6, 2166-2171.
[41] K. Fujimoto, K. Nakahama, M. Shidara and H. Kawaguchi, *Langmuir*, 1999, 15, 4630-4635.
[42] A. Ohnuma, E. C. Cho, P. H. C. Camargo, L. Au, B. Ohtani and Y. N. Xia, *J. Am. Chem. Soc.*, 2009, 131, 1352-1353.
[43] J. Yang, L. Levina, E. H. Sargent and S. O. Kelley, *J. Mater. Chem.*, 2006, 16, 4025-4028.
[44] C. Burda, X. Chen, R. Narayanan and M. A. El-Sayed, *Chem. Rev.*, 2005, 105, 1025-1102.
[45] M. P. Pileni, *Nat. Mater.*, 2003, 2, 145-150.
[46] B. Wiley, Y. Sun, B. Mayers and Y. Xia, *Chem. Eur. J.*, 2005, 11, 454-463.
[47] Y. Xia, Y. Xiong, B. Lim and S. Skrabalak, *Angew. Chem. Int. Ed.*, 2009, 48, 60-103.
[48] Y. Xiong and Y. Xia, *Adv. Mater.*, 2007, 19, 3385-3391.
[49] S. Kumar and T. Nann, *Small*, 2006, 2, 316-329.
[50] L. Manna, E. C. Scher and A. P. Alivisatos, *J. Am. Chem. Soc.*, 2000, 122, 12700-12706.
[51] N. Zhao and L. Qi, *Adv. Mater.*, 2006, 18, 359-362.
[52] X. Teng and H. Yang, *Nano Lett.*, 2005, 5, 885-891.
[53] C.-C. Chen, C.-Y. Chao and Z.-H. Lang, *Chem. Mater.*, 2000, 12, 1516-1518.
[54] L. Gou and C. J. Murphy, *Chem. Mater.*, 2005, 17, 3668-3672.
[55] J. Wang, Q. Chen, C. Zeng and B. Hou, *Adv. Mater.*, 2004, 16, 137-140.
[56] R. Buonsanti, V. Grillo, E. Carlino, C. Giannini, M. L. Curri, C. Innocenti, C. Sangregorio, K. Achterhold, F. G. Parak, A. Agostiano and P. D. Cozzoli, *J. Am. Chem. Soc.*, 2006, 128, 16953-16970.
[57] A. Figuerola, A. Fiore, R. Di Corato, A. Falqui, C. Giannini, E. Micotti, A. Lascialfari, M. Corti, R. Cingolani, T. Pellegrino, P. D. Cozzoli and L. Manna, *J. Am. Chem. Soc.*, 2008, 130, 1477-1487.
[58] T. Pellegrino, A. Fiore, E. Carlino, C. Giannini, P. D. Cozzoli, G. Ciccarella, M. Respaud, L. Palmirotta, R. Cingolani and L. Manna, *J. Am. Chem. Soc.*, 2006, 128, 6690-6698.
[59] L. Carbone, S. Kudera, C. Giannini, G. Ciccarella, R. Cingolani, P. D. Cozzoli and L. Manna, *J. Mater. Chem.*, 2006, 16, 3952-3956.

[60] J. Yang, J. Peng, Q. Zhang, F. Peng, H. Wang and H. Yu, *Angew. Chem.*, 2009, 121, 4051-4055.
[61] H. Gu, Z. Yang, J. Gao, C. K. Chang and B. Xu, *J. Am. Chem. Soc.*, 2005, 127, 34-35.
[62] M. Haruta, T. Kobayashi, H. Sano and N. Yamada, *Chem. Lett.*, 1987, 405-408.
[63] Z.-P. Liu, X.-Q. Gong, J. Kohanoff, C. Sanchez and P. Hu, *Phys. Rev. Lett.*, 2003, 91, 266102.
[64] A. Bulgac, M. M. Forbes and A. Schwenk, *Phys. Rev. Lett.*, 2006, 97, 020402.
[65] R. Paiva and R. D. Felice, *ACS Nano*, 2008, 2, 2225-2236.
[66] N. Liu, B. S. Prall and V. I. Klimov, *J. Am. Chem. Soc.*, 2006, 128, 15362-15363.
[67] W. Zhang, Y. Lu, T. Zhang, W. Xu, M. Zhang and S. Yu, *J. Phys. Chem. C*, 2008, 112, 19872-19877.
[68] M. Cheng, S. Liu, H. Zhou, Z. Hao and Q. Wang, *Opt. Lett.*, 2007, 32, 2125-2127.
[69] T. Young, *Philosophical Transactions of the Royal Society of London*, 1805, 95, 65-87.
[70] J. W. Mullin, *Crystallization*, Butterworth-Heinemann, Oxford, 2001.
[71] M. Volmer, *Z. Electrochem.*, 1929, 35, 555.
[72] M. Volmer, *Kinetic der Phasebildung*, Steinkopf, Dresden, 1939.
[73] E. V. Khamskii, *Crystallization from solutions*, Consultants bureau, New York, 1969.
[74] O. Söhnel and J. W. Mullin, *J. Cryst. Growth*, 1978, 44, 377-382.
[75] X. Y. Liu, *J. Chem. Phys.*, 2000, 112, 9949-9955.
[76] V. K. LaMer and R. H. Dinegar, *J. Am. Chem. Soc.*, 1950, 72, 4847-4854.
[77] V. P. Skripov, *Current Topics in Material Science*, North-Holland, Amsterdam, 1977.
[78] A. A. Chernov, *Modern Crystallography III - Crystal Growth*, Springer, Berlin, 1984.
[79] B. Mutaftschiev, *Handbook on Crystal Growth*, North-Holland, Amsterdam, 1993.
[80] P. S. R. Lacmann, *Current Topics in Materials Science*, North-Holland, Amsterdam, 1977.
[81] S. A. Chambers, *Surf. Sci. Rep.*, 2000, 39, 105-180.
[82] Z. Peng, H. Yang, *Nano Today*, 2009, 4, 143-164.
[83] D. J. Eaglesham and M. Cerullo, *Phys. Rev. Lett.*, 1990, 64, 1943.
[84] Y. W. Mo, D. E. Savage, B. S. Swartzentruber and M. G. Lagally, *Phys. Rev. Lett.*, 1990, 65, 1020.
[85] B. Voigtlander and A. Zinner, *Appl. Phys. Lett.*, 1993, 63, 3055-3057.
[86] S. Guha, A. Madhukar and K. C. Rajkumar, *Appl. Phys. Lett.*, 1990, 57, 2110-2112.
[87] D. Leonard, K. Pond and P. M. Petroff, *Phys. Rev. B*, 1994, 50, 11687-11692.
[88] M. Sopanen, H. Lipsanen and J. Ahopelto, *Appl. Phys. Lett.*, 1995, 67, 3768-3770.
[89] Y. Chen and J. Washburn, *Phys. Rev. Lett.*, 1996, 77, 4046.
[90] F.-R. Fan, D.-Y. Liu, Y.-F. Wu, S. Duan, Z.-X. Xie, Z.-Y. Jiang and Z.-Q. Tian, *J. Am. Chem. Soc.*, 2008, 130, 6949-6951.
[91] K.-C. Huang and S. H. Ehrman, *Langmuir*, 2006, 23, 1419-1426.
[92] W. Ostwald, *Z. Phys. Chem.*, 1897, 22, 289.
[93] W. Ostwald, *Z. Phys. Chem.*, 1900, 34, 495.
[94] *IUPAC Compendium of Chemical Terminology, 2nd Edition*, 1997.
[95] P. D. Cozzoli and L. Manna, *Nat. Mater.*, 2005, 4, 801-802.
[96] B. Liu and H. C. Zeng, *Small*, 2005, 1, 566-571.
[97] W. J. Plieth, *J. Electroanal. Chem.*, 1986, 204, 343-349.
[98] T. Mokari, C. G. Sztrum, A. Salant, E. Rabani and U. Banin, *Nat. Mater.*, 2005, 4, 855-863.
[99] M. Zinke-Allmang, L. C. Feldman and M. H. Grabow, *Surf. Sci. Rep.*, 1992, 16, 377-463.

[100] H. Yu, M. Chen, P. M. Rice, S. X. Wang, R. L. White and S. Sun, *Nano Lett.*, 2005, 5, 379-382.
[101] T. D. Schladt, M. I. Shukoor, K. Schneider, M. N. Tahir, F. Natalio, I. Ament, J. Becker, F. D. Jochum, S. Weber, O. Köhler, P. Theato, L. M. Schreiber, C. Sönnichsen, H. C. Schröder, W. E. G. Müller and W. Tremel, *Angew. Chem. Int. Ed.*, 2010, 49, 3976-3980.
[102] H. Gu, R. Zheng, X. Zhang and B. Xu, *J. Am. Chem. Soc.*, 2004, 126, 5664-5665.
[103] F. Wang and W. E. Buhro, *J. Am. Chem. Soc.*, 2007, 129, 14381-14387.
[104] J. Zeng, J. Huang, C. Liu, C. H. Wu, Y. Lin, X. Wang, S. Zhang, J. Hou and Y. Xia, *Adv. Mater.*, 2010, 22, 1936-1940.
[105] S. Chakrabortty, Jie A. Yang, Yee M. Tan, N. Mishra and Y. Chan, *Angew. Chem. Int. Ed.*, 2010, 49, 2888-2892.
[106] G. Menagen, J. E. Macdonald, Y. Shemesh, I. Popov and U. Banin, *J. Am. Chem. Soc.*, 2009, 131, 17406-17411.
[107] A. E. Saunders, I. Popov and U. Banin, *J. Phys. Chem. B*, 2006, 110, 25421-25429.
[108] T. Mokari, A. Aharoni, I. Popov and U. Banin, *Angew. Chem. Int. Ed.*, 2006, 45, 8001-8005.
[109] J. Yang, E. Sargent, S. Kelley and J. Y. Ying, *Nat. Mater.*, 2009, 8, 683-689.
[110] H. Gu, Z. Yang, J. Gao, C. K. Chang and B. Xu, *J. Am. Chem. Soc.*, 2005, 127, 34-35.
[111] L. Zhang, Y.-H. Dou and H.-C. Gu, *J. Colloid Interface Sci.*, 2006, 297, 660-664.
[112] W. Shi, H. Zeng, Y. Sahoo, T. Y. Ohulchanskyy, Y. Ding, Z. L. Wang, M. Swihart and P. N. Prasad, *Nano Lett.*, 2006, 6, 875-881.
[113] Y. Wei, R. Klajn, A. O. Pinchuk and B. A. Grzybowski, *Small*, 2008, 4, 1635-1639.
[114] Y. Lee, M. A. Garcia, N. A. F. Huls, S. Sun, *Angew. Chem. Int. Ed.*, 2010, 49, 1271-1274.
[115] K. W. Kwon and M. Shim, *J. Am. Chem. Soc.*, 2005, 127, 10269-10275.
[116] L. Qu and X. Peng, *J. Am. Chem. Soc.*, 2002, 124, 2049-2055.
[117] J. Zeng, W. Lu, X. Wang, B. Wang, G. Wang and J. G. Hou, *J. Colloid Interface Sci.*, 2006, 298, 685-688.
[118] J. Zeng, C. Liu, J. Huang, X. Wang, S. Zhang, G. Li and J. Hou, *Nano Lett.*, 2008, 8, 1318-1322.
[119] W. Lu, B. Wang, J. Zeng, X. Wang, S. Zhang and J. G. Hou, *Langmuir*, 2005, 21, 3684-3687.
[120] X. Lu, H.-Y. Tuan, Brian A. Korgel and Y. Xia, *Chem. Eur. J.*, 2008, 14, 1584-1591.
[121] Z. Li, J. Tao, X. Lu, Y. Zhu and Y. Xia, *Nano Lett.*, 2008, 8, 3052-3055.
[122] X. Lu, M. S. Yavuz, H.-Y. Tuan, B. A. Korgel and Y. Xia, *J. Am. Chem. Soc.*, 2008, 130, 8900-8901.
[123] Z. Li, W. Li, Pedro H. C. Camargo and Y. Xia, *Angew. Chem.*, 2008, 120, 9799-9802.
[124] T. K. Sau and C. J. Murphy, *Langmuir*, 2004, 20, 6414-6420.
[125] B. Nikoobakht and M. A. El-Sayed, *Chem. Mater.*, 2003, 15, 1957-1962.
[126] S. U. Son, I. K. Park, J. Park and T. Hyeon, *Chem. Comm.*, 2004, 778-779.
[127] S. Kudera, L. Carbone, M. F. Casula, R. Cingolani, A. Falqui, E. Snoeck, W. J. Parak and L. Manna, *Nano Lett.*, 2005, 5, 445-449.
[128] S. E. Habas, P. Yang and T. Mokari, *J. Am. Chem. Soc.*, 2008, 130, 3294-3295.
[129] M. T. Sheldon, P. E. Trudeau, T. Mokari, L. W. Wang, A. P. Alivisatos, *Nano Lett.*, 2009, 9, 3676-3682.
[130] R. Glass, M. Moller and J. P. Spatz, *Nanotech.,* 2003, 14, 1153-1160.

[131] Y. Wei, K. Bishop, J. Kim, S. Soh and B. Grzybowski, *Angew. Chem. Int. Ed.*, 2009, 48, 9477-9480.
[132] R. Costi, A. E. Saunders and U. Banin, *Angew. Chem. Int. Ed.*, 2010, 49, 4878-4897.

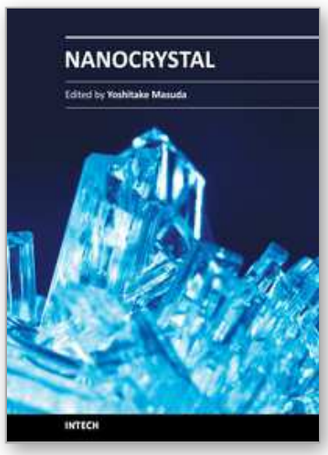

Nanocrystal

Edited by Dr. Yoshitake Masuda

ISBN 978-953-307-199-2
Hard cover, 494 pages
Publisher InTech
Published online 28, June, 2011
Published in print edition June, 2011

We focused on cutting-edge science and technology of Nanocrystals in this book. â€œNanocrystalâ€ is expected to lead to the creation of new materials with revolutionary properties and functions. It will open up fresh possibilities for the solution to the environmental problems and energy problems. We wish that this book contributes to bequeath a beautiful environment and valuable resources to subsequent generations.

How to reference

In order to correctly reference this scholarly work, feel free to copy and paste the following:

Jie Zeng, Xiaoping Wang and J. G. Hou (2011). Colloidal Hybrid Nanocrystals: Synthesis, Properties, and Perspectives, Nanocrystal, Dr. Yoshitake Masuda (Ed.), ISBN: 978-953-307-199-2, InTech, Available from: http://www.intechopen.com/books/nanocrystal/colloidal-hybrid-nanocrystals-synthesis-properties-and-perspectives

INTECH
open science | open minds

InTech Europe
University Campus STeP Ri
Slavka Krautzeka 83/A
51000 Rijeka, Croatia
Phone: +385 (51) 770 447
Fax: +385 (51) 686 166
www.intechopen.com

InTech China
Unit 405, Office Block, Hotel Equatorial Shanghai
No.65, Yan An Road (West), Shanghai, 200040, China
中国上海市延安西路65号上海国际贵都大饭店办公楼405单元
Phone: +86-21-62489820
Fax: +86-21-62489821

IntechOpen